

Whispering gallery mode lasing in high quality GaAs/AlAs pillar microcavities

P. Jaffrennou,¹ J. Claudon,^{1,a)} M. Bazin,¹ N. S. Malik,¹ S. Reitzenstein,² L. Worschech,² M. Kamp,² A. Forchel,² and J.-M. Gérard¹

¹CEA-CNRS-UJF group "Nanophysique et Semiconducteurs," CEA, INAC, SP2M, F-38054 Grenoble, France

²Technische Physik, Physikalisches Institut and Wilhelm Conrad Röntgen Research Center for Complex Material Systems, Universität Würzburg, Am Hubland, D-97074 Würzburg, Germany

(Received 24 November 2009; accepted 22 January 2010; published online 17 February 2010)

We report whispering gallery mode (WGM) lasing from high quality GaAs/AlAs micropillars with embedded InAs quantum dots, under continuous optical pumping. For temperatures ranging from 5 to 100 K, simultaneous lasing from $TE_{1,1,m}$ WGMs is observed for pillar diameters in the 3–4 μm range. Spectral linewidths and energy shifts of the lasing modes are analyzed as a function of the pump power. Thanks to the efficient heat sinking provided by the micropillar geometry, a clear line narrowing is observed above threshold. Moreover, the lasing mode energy remains stable for pump power as large as six times the lasing threshold. © 2010 American Institute of Physics.

[doi:10.1063/1.3315869]

Semiconductor microdisk cavities support high-Q and low mode volume whispering gallery modes (WGM). Taking advantage of these appealing figures of merit, low threshold WGM microlasers have been demonstrated using quantum wells^{1,2} or quantum dots (QD) (Refs. 3–6) as a gain medium. Recently, light extraction from a microdisk by an integrated waveguide has been demonstrated,⁷ showing the potential of WGM lasers as internal light sources for integrated planar photonic circuits. Alternatively, out of plane emission can be achieved by patterning a proper grating on top of the resonator.⁸

So far, most of the semiconductor microdisk resonators are air-cladded structures supported by a semiconductor pedestal with a lower diameter.⁹ This approach provides a limited heat sinking which leads to a marked temperature increase in the microdisk periphery under strong pumping.¹⁰ As a consequence, the lasing modes in microdisks usually show a pronounced thermal redshift⁹ and limited spectral narrowing above threshold. Bonding directly the microdisk on a sapphire wafer improves significantly heat evacuation¹⁰ but complicates the implementation of electrical pumping in a practical device.

Following the fast improvements in the fabrication of GaAlAs micropillars,¹¹ it was recently shown that these cavities support high-Q WGMs which are located on the circumference of the central GaAs layer.^{12,13} In this letter, we report on a WGM laser based on this micropillar geometry. The semiconductor pedestal, which is as large as the microdisk area, provides a very efficient heat sinking, a crucial asset for operation well above the lasing threshold. Under continuous optical pumping, the lasing modes experience a marked spectral narrowing that maintains for pumping power six times above the lasing threshold. Moreover, the lasing modes also demonstrate spectral stability with a limited thermal redshift. Combined with an easier electrical charge injection in the pillar geometry,¹⁴ these results open appealing prospects for the development of high performance semiconductor WGM microlasers.

As detailed in Ref. 13, our micropillar sample is etched from a planar cavity grown by molecular beam epitaxy. The central 290-nm-thick GaAs layer is sandwiched between a bottom and a top distributed Bragg reflector (DBR), respectively composed of 27 and 17 AlAs/GaAs periods. The optical gain is provided by three arrays of self-assembled InAs QDs embedded in the GaAs cavity as follows: two of them are located 10 nm away from the center and the third one 20 nm away from the bottom DBR. Their fundamental optical transition peaks at 1.27 eV with an inhomogeneous width of about 40 meV.

The photoluminescence (PL) spectra of individual micropillars were recorded with a μPL setup featuring a variable-temperature helium flow cryostat. Carrier injection in the QDs is provided by a cw Ti:Sapphire laser focused on the sample with a microscope objective (NA=0.4). The same objective collects the luminescence signal which is dispersed by a spectrometer and detected by a nitrogen-cooled charge coupled device camera. The spectral resolution of the setup is 40 μeV . To efficiently collect the far-field emission of WGMs, the sample was mounted on a 45° tilted sample holder [Fig. 1(a)]. The excitation laser was tuned below the GaAs band gap, on resonance with the wetting layer (1.47 eV) in order to ensure a homogeneous excitation of the QDs. The fraction of light absorbed by the gain medium is on the order of a few percent. However, given the uncertainties on this estimation, we use in the following the as-measured external pump power P .

Figure 1(b) displays typical PL spectra of a 4 μm diameter micropillar, recorded at 5 K. The spectra are dominated by regularly spaced, sharp lines associated to the $TE_{1,1,m}$ mode family. Following Ref. 13, the azimuthal index m of the modes is identified using an effective index theory. While doubly degenerate WGMs are predicted by theory, some modes are split in experiment [Fig. 1(d)], likely because of subwavelength scattering centers that couple counter-propagating WGMs and lift the associated $\pm m$ twofold degeneracy.¹⁵ Such centers could be found on the cavity surface, because of etching imperfections. Alternatively, as pointed in Ref. 16, QDs themselves constitute a perturbation

^{a)}Electronic mail: julien.claudon@cea.fr.

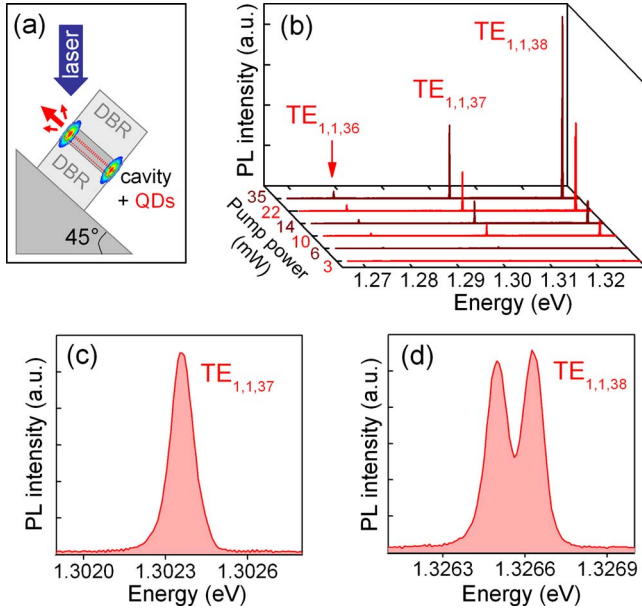


FIG. 1. (Color online) Lasing of micropillar WGMs. (a) Sketch of the micropillar structure and tilted geometry of the μ PL experiment. (b) PL spectra of a $4\text{-}\mu\text{m}$ -diameter micropillar at $T=5\text{ K}$ for pump power P ranging from 3 to 35 mW. (c) and (d) Zooms of the $\text{TE}_{1,1,m}$ lasing modes for $P=10.5\text{ mW}$.

of the refractive index inside the cavity that could lift the $\pm m$ degeneracy.

When the pumping power increases, the broadband inhomogeneous gain of QDs allows simultaneous lasing of WGMs. In Fig. 1(b), the $\text{TE}_{1,1,38}$ and $\text{TE}_{1,1,37}$ modes, which are coupled to P-shell QD transitions, show the unambiguous signature of lasing. On the low energy side of the spectrum, the $\text{TE}_{1,1,36}$ mode, coupled to S-shell transitions, experiences a smaller gain and the associated PL intensity saturates. Such a multimode lasing behavior has been observed for various pillars with diameters from 3 to 4 μm . Lasing has been observed up to 100 K. Above this temperature, the optical gain becomes too small, because of thermal activation which spills the carriers out of the QDs. This can be overcome by increasing the number of QD layers and/or using QDs with a higher confinement energy.⁵

In the following, we investigate the laser performance of these micropillars at 5 K. We focus on the split mode $\text{TE}_{1,1,38}$ that can be fit to a double Lorentzian lineshape up to $P=40\text{ mW}$, and analyze the output intensity, linewidth, and mode energy as a function of P .

The input-output characteristic of this mode is plotted in log-log scale in Fig. 2. Above a threshold pump power $P_{th}=7\text{ mW}$, a superlinear increase in the output power indicates the onset of lasing. The experimental full width at half maximum (FWHM) ΔE is shown in Fig. 3(a). For $P \ll P_{th}$, the linewidth is dominated by QD absorption and exceeds the bare cavity linewidth $\Delta E_c=260\text{ }\mu\text{eV}$ which corresponds to $Q_c=5000$.¹⁷ Above threshold, stimulated emission dominates and ΔE decreases down to $70\text{ }\mu\text{eV}$, which represents a spectral narrowing by a factor of 3 as compared to the bare cavity linewidth. Moreover, this narrow lineshape is maintained for P up to $6P_{th}$. This is a clear improvement over previous demonstration of QD WGM microlasers, where ΔE remains constant or broadens above threshold.³⁻⁶ For $P > 40\text{ mW}$, the lineshape becomes progressively Gaussian

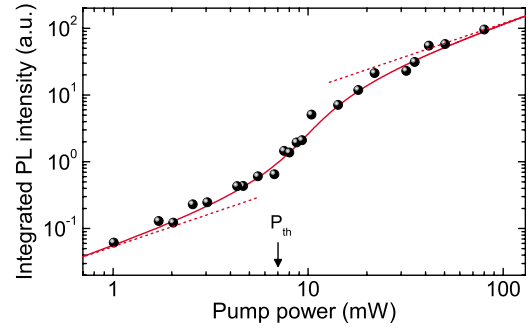


FIG. 2. (Color online) Input-output characteristic of the $\text{TE}_{1,1,38}$ mode at $T=5\text{ K}$ (double logarithmic scale). The experimental integrated PL intensity (points) is fit to Eq. (1) (solid line).

and ΔE increases (not shown here). Since this is correlated with the appearance of a thermal redshift of the mode (see the discussion in the end of the paper), this can be attributed to the heating of the system.

To provide a quantitative insight on the system parameters, we adopt a simple rate equation model. The QDs are considered as two-level systems¹⁸ and ΔE is calculated following Ref. 19, taking into account the absorption of empty QDs. Denoting \bar{n} the mean photon number in the cavity and p the pumping rate of the QD excited state, we have the following expressions:

$$p = \frac{\Gamma_c}{\beta} [1 + 2\xi + 2\beta(\bar{n} - \xi)] \frac{\bar{n}}{1 + 2\bar{n}}, \quad (1)$$

$$\Delta E = \hbar \Gamma_c \frac{1 + 2\xi}{1 + 2\bar{n}}. \quad (2)$$

Here, Γ_c is the photon escape rate from the bare cavity, β is the fraction of QD spontaneous emission (SE) funneled into

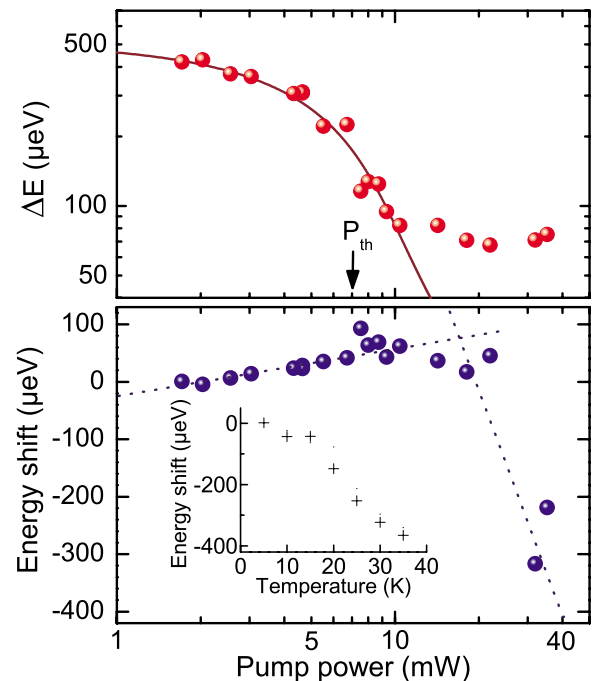


FIG. 3. (Color online) Spectral characteristics of the $\text{TE}_{1,1,38}$ lasing mode at 5 K. (a) FWHM (circles) as a function of the pump power; the solid curve is the prediction using Eq. (2). (b) Energy shift of the mode (circles). The dashed lines are guides for the eye. Inset: Energy shift vs cryostat temperature.

the cavity mode; ξ represents the mean number of SE photons in the cavity at the gain medium transparency.

The input-output characteristic is well reproduced with $\beta=0.075$, $\xi=0.46$, and $\hbar\Gamma_c=\Delta E_c=260 \mu\text{eV}$. The experimental β factor is much smaller than the estimation $\bar{F}_p/(\bar{F}_p+1)=0.7$, where $\bar{F}_p=2.5$ is the spatially and spectrally averaged Purcell factor for an inhomogeneous ensemble of monochromatic emitters.²⁰ This points toward a QD line-shape homogeneous broadening in the 10 meV range, which is typical for strong nonresonant pumping.²¹

The theoretical description of the mode linewidth is in good agreement with the experimental data for $P < P_{th}$. However, for high pumping power, the experimental data shows a saturation and deviates from the Schawlow–Townes prediction ($\Delta E \propto 1/\bar{n}$ for $\bar{n} \gg 1$).²² Such a plateau in the linewidth can be explained with a microscopic description of the gain medium fluctuations,² which is beyond the scope of this work.

Finally, we study the evolution of the mode energy, which is a very sensitive probe of the cavity temperature. Taking the lowest power measurement as a reference, the shift in the mode energy is plotted against P in Fig. 3(b). Note that we discuss here small shifts, of about a few hundred μeV . Below threshold, the linear blueshift is attributed to the increase in the free carrier concentration in the wetting layer. Around threshold, the energy mode reaches a plateau followed by a redshift, associated with heating effects. To estimate the structure temperature, we have measured the mode energy for increasing cryostat temperature, using a low pumping power ($P < 1 \text{ mW}$). Taking the 5 K measurements as a reference, the thermal mode shift is shown in the insert in Fig. 3(b). The comparison to Fig. 3(b) shows that $T < 15 \text{ K}$ for $P < 3P_{th}$. The last experimental point ($P=6P_{th}$) corresponds to $T \sim 35 \text{ K}$. We attribute this remarkable thermal stability to the efficient heat sinking associated to the micropillar geometry.

In summary, we have investigated the lasing properties of high-Q WGM pillar microcavities. Thanks to the efficient heat sinking provided by the pillar geometry, the lasing mode demonstrates a stable emission wavelength and a marked spectral narrowing above threshold. These appealing spectral properties, combined with an easier electrical charge injection in the pillar geometry¹⁴ are promising for the realization of practical, high performance WGM lasers. Spectral purity and stable mode energy well above lasing threshold are particularly relevant for a recently proposed WGM terahertz source.²³

The authors acknowledge Y.-R. Nowicki-Bringuier, M. Emmerling, and A. Wolf for expert sample preparation. This work was supported by the European Commission through the IST STREP Project No. 29283 'QPhoton'. J.C., N.S.M. and J.M.G. acknowledge financial support from the foundation 'Nanoscience aux limites de la Nanoélectronique'.

¹S. L. McCall, A. F. J. Levi, R. E. Slusher, S. J. Pearton, and R. A. Logan, *Appl. Phys. Lett.* **60**, 289 (1992).

²U. Mohideen, R. E. Slusher, F. Jahnke, and S. W. Koch, *Phys. Rev. Lett.* **73**, 1785 (1994).

³H. Cao, J. Y. Xu, W. H. Xiang, Y. Ma, S.-H. Chang, S. T. Ho, and G. S. Solomon, *Appl. Phys. Lett.* **76**, 3519 (2000).

⁴P. Michler, A. Kiraz, C. Becher, L. Zhang, E. Hu, A. Imamoglu, W. V. Schoenfeld, and P. Petroff, *Phys. Status Solidi B* **224**, 797 (2001).

⁵T. Ide, T. Baba, J. Tatebayashi, S. Iwamoto, T. Nakaoka, and Y. Arakawa, *Appl. Phys. Lett.* **85**, 1326 (2004).

⁶E. Peter, I. Sagnes, G. Guirleo, S. Varoutsis, J. Bloch, A. Lemaître, and P. Senellart, *Appl. Phys. Lett.* **86**, 021103 (2005).

⁷S. Koseki, B. Zhang, K. D. Greve, and Y. Yamamoto, *Appl. Phys. Lett.* **94**, 051110 (2009).

⁸L. Mahler, A. Tredicucci, F. Beltram, C. Walther, J. Faist, B. Witzigmann, H. E. Beere, and D. A. Ritchie, *Nat. Photonics* **3**, 46 (2008).

⁹B. Gayral, J. M. Gérard, A. Lemaître, C. Dupuis, L. Manin, and J. L. Pelouard, *Appl. Phys. Lett.* **75**, 1908 (1999).

¹⁰S. M. K. Thiyagarajan, A. F. J. Levi, C. K. Lin, I. Kim, P. D. Dapkus, and S. J. Pearton, *Electron. Lett.* **34**, 2333 (1998).

¹¹S. Reitzenstein, C. Hofmann, A. Gorbunov, M. Strauß, S. H. Kwon, C. Schneider, A. Löffler, S. Höfling, M. Kamp, and A. Forchel, *Appl. Phys. Lett.* **90**, 251109 (2007).

¹²V. Astratov, S. Yang, S. Lam, B. D. Jones, D. Sanvitto, D. M. Whittaker, A. M. Fox, M. S. Skolnick, A. Tahraoui, P. W. Fry, and M. Hopkinson, *Appl. Phys. Lett.* **91**, 071115 (2007).

¹³Y.-R. Nowicki-Bringuier, J. Claudon, C. Böckler, S. Reitzenstein, M. Kamp, A. Morand, A. Forchel, and J. Gérard, *Opt. Express* **15**, 17291 (2007).

¹⁴C. Böckler, S. Reitzenstein, C. Kistner, R. Debusmann, A. Löffler, T. Kida, S. Höfling, A. Forchel, L. Grenouillet, J. Claudon, and J. M. Gérard, *Appl. Phys. Lett.* **92**, 091107 (2008).

¹⁵A. Mazzei, S. Götzinger, L. de S. Menezes, G. Zumofen, O. Benson, and V. Sandoghdar, *Phys. Rev. Lett.* **99**, 173603 (2007).

¹⁶K. R. Hiremath and V. N. Astratov, *Opt. Express* **16**, 5421 (2008).

¹⁷ Q_c is estimated considering the nonlasing $\text{TE}_{1,1,36}$ mode. Denoting Q_0 (resp. Q_∞) the $P \rightarrow 0$ (resp. $P \rightarrow \infty$) Q -factor, $2Q_c^{-1} = Q_0^{-1} + Q_\infty^{-1}$. $Q_c = 5000$ is obtained with this method, and confirmed by the theoretical analysis detailed in the paper.

¹⁸J.-M. Lourtioz, H. Benisty, V. Berger, J.-M. Gérard, D. Maustre, and A. Tchebnokov, *Photonic Crystals*, 2nd ed. (Springer, New York, 2008).

¹⁹G. Bjork and Y. Yamamoto, *IEEE J. Quantum Electron.* **27**, 2386 (1991).

²⁰B. Gayral, *Ann. Geophys. (France)* **26**, 1 (2001).

²¹P. Borri, W. Langbein, J. M. Hvam, F. Heinrichsdorff, M.-H. Mao, and D. Bimberg, *Appl. Phys. Lett.* **76**, 1380 (2000).

²²A. L. Schawlow and C. H. Townes, *Phys. Rev.* **112**, 1940 (1958).

²³A. Andronico, J. Claudon, J.-M. Gérard, V. Berger, and G. Leo, *Opt. Lett.* **33**, 2416 (2008).